Flux Calculation in HKKM

Morihiro HONDA
Institute for Cosmic Ray Research, University of Tokyo, 5-1-5 Kashiwa-no-Ha, Kashiwa City, Chiba 277-8582, Japan

Abstract

The calculation of atmospheric neutrino flux in HKKM04 [1] is over viewed. There are many improvements from HKKM95 [2]; the primary flux model is replaced by the one based on the AMS [3] and BESS [4] observations, and the interaction model is changed to DPMJET-III [5]. Also the calculation is carried out in a full 3-dimensional scheme. However, the differences between 3D and 1D calculations are not seen in the averaged fluxes over the azimuthal angles for $\gtrsim$ 3 GeV.

1. Introduction

The study of atmospheric neutrinos is carried out by the comparison of theoretical prediction and experimental observation for the atmospheric neutrinos. As the SuperKamiokande is steadily improving the statistics and the accuracy of observed atmospheric neutrino data, it is important to improve the theoretical prediction for them.

Since our former comprehensive study HKKM95 [2] was completed, the knowledge of the primary cosmic ray is largely improved by the precise measurements, such as AMS [3] and BESS [4] below 100 GeV. There are also theoretical developments in hadronic interaction models, such as Fritiof 7.02 [6], FLUKA97 [7] and DPMJET-III [5]. These progresses are taken into HKKM04 [1].

We also have developed a new and fast simulation code for the propagation of cosmic rays in the atmosphere, in order to calculate the atmospheric neutrino flux in a full 3-dimensional scheme without assuming a symmetry. This fast simulation code and a fast computer system allow us to calculate the atmospheric neutrino flux with a good accuracy over the wide energy region from 0.1 to a few 10 GeV. Then the differences of the neutrino fluxes between 3d and 1d calculations are precisely studied. The neutrino flux calculated in the 3-dimensional scheme is smoothly connected to the one calculated in the 1-dimensional scheme at a few

pp. 101–107

10 GeV, but we limit this overview for neutrinos below 30 GeV.

2. Primary cosmic ray flux model

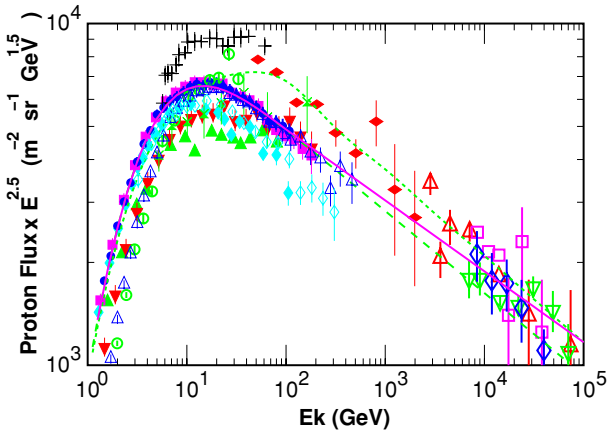

Fig 1. The data and models for the primary cosmic ray protons. Closed circles stand for BESS [4], closed horizontal diamonds AMS [3], and open upward triangle BESS-TeV [8]. For other data points, see Fig. 1 of HKKM04. The solid line is the proton flux model in HKKM04, the dotted line in HKKM95, and dashed line in Refs. [9] and [10]. The model curves are for the solar minimum.

The primary flux model is based on Refs. [9] and [10], in which the cosmic ray data below 100 GeV were compiled. However, the extension of the flux model for cosmic ray protons does not agree with emulsion chamber experiments above ~ 10 TeV (the dashed line in Fig. 1). We modified the power index above 100 GeV to -2.71 in HKKM04, so that the extension passes through the center of the emulsion chamber data (the solid line in Fig. 1). The flux model for cosmic ray protons used in HKKM95 is also shown by the dotted line in Fig. 1. Other than the cosmic ray protons, we use the same flux models as in Ref. [10]. Note, there are differences in the flux model for nuclear cosmic rays heavier than He between Refs. [9] and [10],

3. Hadronic Interaction Model

We are using theoretically constructed hadronic interaction models, which have been successfully applied to the high energy accelerator experiments. After publication of HKKM95, there were almost no improvements in the experimental study of the multiple production in the hadron interactions, but there are noticeable improvements in the theoretical study, resulting in Fritiof 7.02 [6], FLUKA97 [7], and DPMJET-III [5].

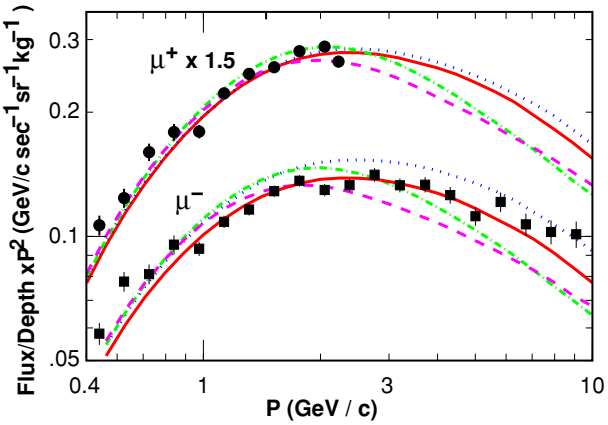

Fig 2. The quantity $[Flux/Depth]$ averaged over all the muon observation by BESS 2001 [12] at balloon altitudes. The lines are the same quantities calculated by DPMJET-III (Solid line), Fritiof 1.6 (Dashed line), Fritiof 7.02 (dotted line), and FLUKA 97 (Dash dot),

To select a better interaction model, we have used the secondary cosmic rays at the balloon altitude. The fluxes of secondary cosmic rays at balloon altitude are ideal material for this study. They are approximately proportional to the air depth, and the ratio $[Flux/Depth]$ is determined almost only by the interaction and the flux of primary cosmic rays. In Fig.2, we show a study on the muon observation at balloon altitude by BESS 2001 [11]. Although it is hard to discriminate other interaction models, it is found the DPMJET-III gives the best agreement between calculation and observation (for details, see Ref. [12]) for 0.4 – 10 GeV/c in muon momentum, roughly corresponding to 0.3 – 3 GeV in the neutrino energy.

We do not use the original package of the hadronic interaction code in the calculation of atmospheric neutrino fluxes. From the output of the interaction model, we construct an inclusive interaction code which reproduces the multiplicities and energy spectra of secondary particles as the original code. The inclusive interaction code violates the conservation laws in a single interaction, but they are restored statistically. Therefore, the inclusive interaction code is only valid for the calculation of a time averaged quantity, such as the fluxes of atmospheric muons and neutrinos. However, the inclusive codes are typically $\sim$100 times faster than the original package. The fast computation is very important in the 3-dimensional calculation of the atmospheric neutrino fluxes, as well as for the study of secondary cosmic rays.

4. Calculation Scheme

We assume the surface of the Earth is a sphere with the radius R_e = 6378.180 km. We consider 3 more spheres, injection, simulation, and escape spheres. The radius of the injection sphere is taken as $R_{inj} = R_e + 100$ km, the simulation sphere $R_{sim} = R_e + 3000$ km, and the escape sphere $R_{esc} = 10 \times R_e$.

The rigidity cutoff test is carried out between the injection sphere and the escape sphere. When a cosmic ray passed through the test, it is fed to the simulation code. Then, the all particle propagations, including that for the cosmic ray and those for secondary particles, are simulated in the space between the surface of Earth and the simulation sphere, until all the particle reach the boundary or decay, or the energies become lower than the interaction threshold for stable particles. Note, when a particle other than the neutrinos enters the Earth, it loses its energy very quickly, and can create low energy neutrinos ($\lesssim 0.1$ GeV) only in the Earth.

Note, too small size simulation sphere causes an error in the neutrino fluxes. We have examined proper size for the simulation sphere in HKKM04, and find the simularion sphere defined above does not cause an error larger than 1 %.

For the atmosphere model, we use US-standard '76 [13]. This model is a good approximation for the one year averaged atmosphere, in the comparison with the newer atmosphere models [14]. For the geomagnetic field model, we use the IGRF geomagnetic field model [15] with the 10th order expansion by the spherical function for the year 2000. As the geomagnetic field changes very slowly, the neutrino flux calculated for the year 2004 would not show a noticeable difference.

For the observation of neutrinos. we use a virtual detector, the surface of the Earth inside a circle with the radius of ~ 1117 km (center angle of 10°) around the target detector. Note, too large virtual detector is a source of the calculation errors. We have studied the errors comes from the large size virtual detector, and find the error is reasonably small [16] with the above virtual detector.

5. Flux of Atmospheric Neutrinos

We have simulated $\sim$ 300 G cosmic rays with $E_k/A > 1$ GeV after the rigidity cutoff for $\lesssim 10$ GeV, and $\sim$ 400 G cosmic rays with $E_k/A > 10$ GeV for neutrino fluxes $\gtrsim 10$ GeV, under the calculation scheme explained above. Now, we present some features the calculated atmospheric neutrino fluxes (3D), with the one calculated in a 1-dimensional scheme (1D), with the same models for the primary cosmic rays and interactions, for comparison. We find the difference

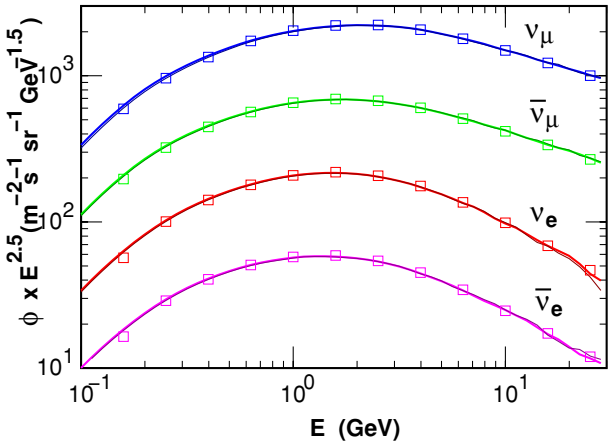

Fig 3. All direction averaged neutrino fluxes. The solid Lines show the results for 3D and the marks for 1D.

between 3D and 1D is small for $\gtrsim$ 0.3 GeV, in Fig. 3.

In Fig. 4, we show the zenith angle dependence of the atmospheric neutrino flux at Kamioka in 3 energy bins, averaging over the azimuth direnctions. There are large difference between 3D and 1D for $\lesssim$ 1 GeV due to the enhancement in 3D for horizontal directions. For vertical directions, 3D's are a little lower than 1D's. However, in the last energy bin, the difference between 3D and 1D is small. Note, the amplitude of the horizontal enhancement is different among different calculations, due to the difference of the $< p_\perp >$ in the interaction models.

In Fig. 5, we depicted the flux ratios, $(\nu_\mu + \bar{\nu}_\mu)/(\nu_e + \bar{\nu}_e)$, $\nu_\mu/\bar{\nu}_\mu$, and $\nu_e/\bar{\nu}_e$. As is reported in many reviews (for example, see Ref. [10]), the raios $(\nu_\mu + \bar{\nu}_\mu)/(\nu_e + \bar{\nu}_e)$ calculated by differenet calculation scheme agrees very will each other in $\lesssim$ 10 GeV. This is because the main source of neutrinos is the $\pi - \mu$ decay in this energy region, and is almost independent of the primary flux and the interaction models. On the other hand the ratios, $\nu_\mu/\bar{\nu}_\mu$ and $\nu_e/\bar{\nu}_e$, are closely related to the interaction model, and the variation among different calculations is larger than the $(\nu_\mu + \bar{\nu}_\mu)/(\nu_e + \bar{\nu}_e)$ ratio.

6. Summary

We have calculated the atmospheric neutrino flux in a full 3-dimensional scheme, with the primary flux model base of the AMS and BESS observations, and the DPMJET-III as the interaction model. In the calculation we simulated around 300 G cosmic rays in the atmosphere for lower energy neutrinos ($\lesssim$ 10 GeV), and around 400 G cosmic rays for higher energy ones ($\gtrsim$ 10 GeV). We estimate the errors come from the calculation scheme and statistics are reasonably small in

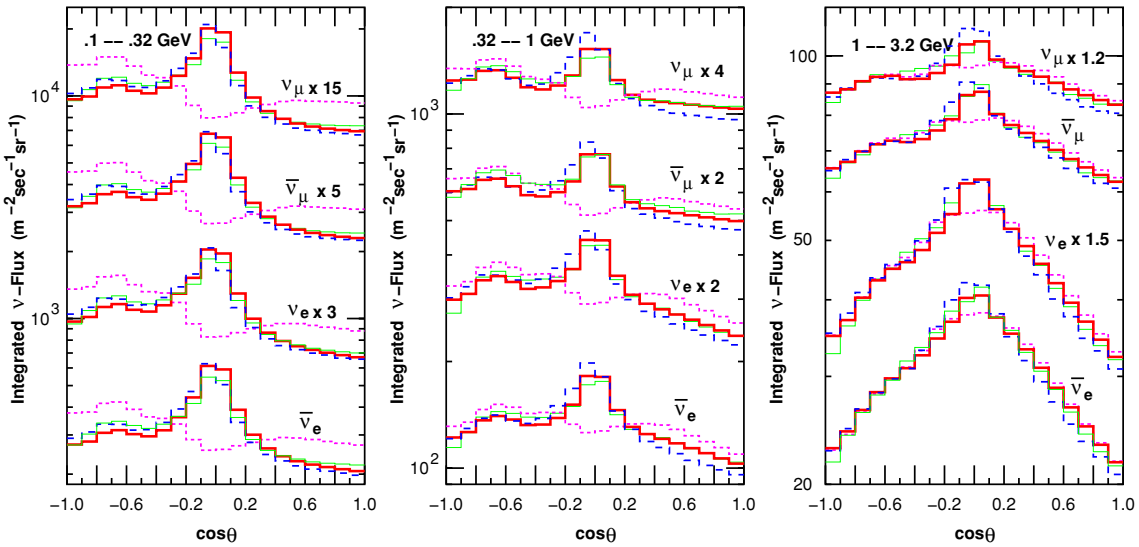

Fig 4. Zenith angle dependence of the atmospheric neutrino flux at Kamioka in 3 energy bins. For the azimuthal directions, averages are taken. The thick solid lines are for 3D, dotted lines for 1D, dashed lines for FLUKA [17], and thin solid lines for DIPOLE [18].

$\lesssim$ 30 GeV (see also Ref. [16]).

The difference between 3d and 1d-calculations are studied in detail. Some muon curvature effect remains up to a few 10 GeV for horizontal directions [1], but most of the differences between 3d and 1d-calculations disappear at a few GeV. The calculated neutrino fluxes are smoothly connected to those calculated in 1-dimensional scheme.

7. Acknowledgments

We are grateful to T. Kajita, K. Kasahara, S. Midorikawa, J. Nishimura, A. Okada, P. Lipari, T. Sanuki, K. Abe, S. Haino, Y. Shikaze and S. Orito for useful discussions and comments. We also thank ICRR, the University of Tokyo, for the support. This study was supported by Grants-in-Aid, KAKENHI(12047206), from the Ministry of Education, Culture, Sport, Science and Technology (MEXT).

References

[1] M. Honda, T. Kajita, K. Kasahara, S. Midorikawa, Phys. Rev. D70:043008 (2004).

[2] M. Honda, T. Kajita, K. Kahahara, S. Midorikawa, Phys. Rev. D54, 4985 (1995).

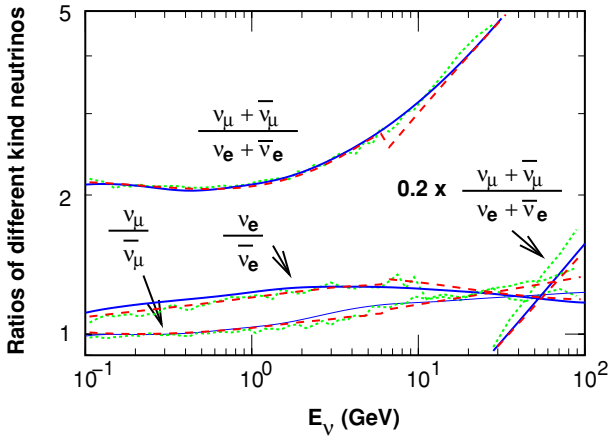

Fig 5. The flux ratio of different kind neutrinos. The solid lines stand for the result of present study, dotted lines for BARTOL[19] and dashed lines for FLUKA[17].

[3] AMS Collaboration: J. Alcaraz et al., Phys. Lett. B 490, 27 (2000).

[4] BESS Collaboration: T. Sanuki et al., Astrophys. J., 545, 1135 (2000).

[5] S. Roesler, R. Engel, and J. Ranft Proc. 27th Int. Cosmic Ray Conf. 1, 439 (2001); Phys. Rev. D 57, 2889 (1998).

[6] Pi H. et al. Comp. Phys. Comm. 71, 173A (1992).

[7] A. Ferrari and P.R. Sala, Trieste, ATLAS internal note ATL-PHYS-97-113 Z1997; Proc. Workshop on Nuclear Reaction Data and Nuclear Reactors Physics, Design and Safety, ICTP, Miramare-Trieste, Italy, 15 April - 17 May 1996. A. Gandini, G. Reffo, eds, Vol. 2 (World Scientific, Singapore, 1998) p. 424.

[8] BESS Collaboration: S. Haino et al., Phys. Lett. B594 35 (2004).

[9] T.K. Gaisser et al., Proc. of the 27th Int. Cosmic Ray Conf. 5, 1643 (2001).

[10] T.K. Gaisser and M. Honda, Ann. Revs. Nucl. Part. Sci. 52, 153 (2002).

[11] BESS Collaboration: K. Abe et al., Phys. Lett. B 564, 8 (2003).

[12] K. Abe et al., Proc. of the 28th Int. Cosmic Ray Conf. 3, 1463 (2003); astro-ph/0312632.

[13] `http://nssdc.gsfc.nasa.gov/space/model/atmos/us_standard.html`.

[14] `http://nssdc.gsfc.nasa.gov/space/model/atmos/msise.html`.

[15] `http://nssdc.gsfc.nasa.gov/space/model/models/igrf.html`.

[16] M. Honda, this conf.

[17] G. Battistoni et al., Astropart. Phys. 12, 315 (2000).

[18] M. Honda, T. Kajita, K. Kasahara, S. Midorikawa, Phys. Rev. D64:053011 (2001).

[19] G.D.Barr, et al., Phys. Rev. D70:023006 (2004)